Astronomy & Astrophysics manuscript no. AA4427c February 3, 2008
(DOI: will be inserted by hand later)

Tertiary companions to close spectroscopic binaries ⋆

A. Tokovinin[1], S. Thomas[1], M. Sterzik[2], S. Udry[3]

[1] Cerro Tololo Inter-American Observatory, Casilla 603, La Serena, Chile
[2] European Southern Observatory, Casilla 19001, Santiago 19, Chile. e-mail: msterzik@eso.org
[3] Observatoire de Genève, CH-1290 Sauverny, Switzerland e-mail: Stephane.Udry@obs.unige.ch

Received / Accepted

Abstract. We have surveyed a sample of 165 solar-type spectroscopic binaries (SB) with periods from 1 to 30 days for higher-order multiplicity. A subsample of 62 targets were observed with the NACO adaptive optics system and 13 new physical tertiary companions were detected. An additional 12 new wide companions (5 still tentative) were found using the 2MASS all-sky survey. The binaries belong to 161 stellar systems; of these 64 are triple, 11 quadruple and 7 quintuple. After correction for incompleteness, the fraction of SBs with additional companions is found to be 63% ± 5%. We find that this fraction is a strong function of the SB period P, reaching 96% for $P < 3^d$ and dropping to 34% for $P > 12^d$. Period distributions of SBs with and without tertiaries are significantly different, but their mass ratio distributions are identical. The statistical data on the multiplicity of close SBs presented in this paper indicates that the periods and mass ratios of SBs were established very early, but the periods of SB systems with triples were further shortened by angular momentum exchange with companions.

Key words. stars: binaries: visual – stars: binaries: spectroscopic – stars: formation

1. Introduction

The formation of binary stars remains a subject of active research and debate (Zinnecker & Mathieu 2001). Close binaries are particularly difficult to explain because at orbital periods of a few days, the separations are less than the size of the individual components during the protostellar phase. Fission of a rapidly rotating pre-main sequence stellar configuration appears unlikely according to the most recent theoretical results (Tohline 2002). Thus, some mechanism(s) of orbit shrinkage must be present in order to extract the angular momentum from a protobinary. This momentum could be deposited in wider stellar companions – a hypothesis we test in this paper.

Stars form in groups and interact dynamically. Detailed studies of dynamical decay of small unstable clusters, e.g. by Sterzik & Durisen (1998), were successful in explaining such properties as multiplicity rate and mass ratio distribution. But dynamical interactions within star clusters alone cannot sufficiently broaden an initially narrow separation distribution (Kroupa & Burkert 2001). Additional dissipative processes and even higher stellar densities are required (Sterzik, Durisen & Zinnecker 2004).

Larson (2002) argues that tidal torques excited by stellar companions in an accretion disk are the most likely and efficient mechanism to extract angular momentum from accreting stars. In the absence of angular momentum transport, accreting matter accumulates in a disk or torus that fragments rapidly, creating the companion. Indeed, hydrodynamical simulations of Bate et al. (2002) show how such companions are formed and how accreting binaries become tighter by interacting with their distant companions or with fly-by members of a nascent cluster. Reipurth (2000) gives convincing evidence that strong accretion and jet activity is actually observed in embedded young multiple systems. He relates periodic knots in Herbig-Haro jets to periastron passages in inner (unresolved) binaries and interprets the decreasing separation between the knots as a fossil record of orbit shrinkage. However, the triple systems examined by Reipurth and Bate et al. are relatively wide systems (∼ 10 A.U.), and cannot account for the characteristics found in short period pre-main-sequence (PMS) spectroscopic binaries (SB). Several PMS binaries with periods shorter than 2 days are known (Melo et al. 2001), and the SB fraction among PMS stars may be as high as among field stars. Many PMS SBs are actually members of higher-order multiple systems (Sterzik et al. 2004). A comprehensive star

Send offprint requests to: A. Tokovinin, e-mail: atokovinin@ctio.noao.edu

⋆ Based on observing runs 74.C-0074 and 75.C-0112 at the Very Large Telescope of the European Southern Observatory at Paranal, Chile. Tables 2 and 5 are only available in electronic form at the CDS via anonymous ftp to cdsarc.u-strasbg.fr (130.79.128.5) or via http://cdsweb.u-strasbg.fr/cgi-bin/qcat?J/A+A/

formation theory must be able to explain these observational facts.

The discovery of massive extrasolar planets with predominantly short orbital periods revived the interest in orbital decay via interactions within disks. Planet migration in a disk is now a generally accepted theory. A distant (stellar) companion enhances planet growth and migration (Zucker & Mazeh 2002; Udry et al. 2003; Eggenberger et al. 2004), possibly in an analogous way to multiple-star formation as envisioned by Larson (2002) and others.

Present-day parameters of close binaries are not identical to their parameters at birth (i.e. when their masses were assembled) because of subsequent evolution. One such evolutionary mechanism is called KCTF – Kozai cycles with tidal friction (Eggleton & Kisseleva-Eggleton 2001). A distant companion in a stable (hierarchical) triple system causes periodic modulation of the inner-binary eccentricity by Kozai cycles. These cycles are periodic, but only as long as the inner system does not interact tidally at periastron. In this case the Kozai cycles are gradually modified, the inner system gets "locked" in a high-eccentricity state and its orbit then slowly decays to a circular SB with a period of few days (Kisseleva et al. 1998). The period distribution of solar-type close binaries within higher-order multiple systems seems to match this scenario, showing a sharp drop in the number of systems with $P > 7^d$ (Tokovinin & Smekhov 2002).

A competing evolutionary effect is the disruption of multiple systems by dynamical instabilities or by perturbations from other stars passing nearby. Thus, SBs formed within higher order multiples can also lose tertiary companions (TCs) at later times. Interactions with field stars can be neglected in the present study because they disrupt only very wide tertiaries with separations above 0.1 pc (see Close et al. 1990 for a review of observational data and theory). Much closer tertiaries with periods as short as ~ 300 yr could be "ionizied" during early evolutionary stages in very young clusters, explaining the difference in wide-binary frequency between young T Tau associations and the field (Kroupa 2001).

Observers have noticed the high multiplicity of close binaries for some time. Mayor & Mazeh (1987) looked for orbital precession (presumably caused by TCs) in a sample of 25 solar-type SBs and found that some 25% of those binaries are triple. Isobe et al. (1992) searched for visual companions to SBs by means of speckle interferometry. Tokovinin (1997, MSC) showed that 43% of nearby solar-type stars with periods under 10 days have known tertiaries. All five such systems in the Duquennoy & Mayor (1991, DM91) G-dwarf sample are triple.

Are *all* close binaries triple? Is the angular momentum of the close binary system always extracted by a tertiary component (via the KCTF mechanism or during accretion)? In the present paper, we attempt an observational investigation of the question and prove that not all close SBs are triple.

The paper is organized as follows. We describe our sample of close solar-type binaries in Sect. 2. New components were discovered with adaptive optics (Sect. 3) and the 2MASS sky survey (Sect. 4). We estimate the massses and periods of all tertiaries in Sect. 5 and describe the detection limits of new and existing techniques in Sect. 6. We study the statistics of tertiary components in Sect. 7. Section 8 summarizes the results, and the implications for close-binary formation theories are discussed in Sect. 9.

2. The sample

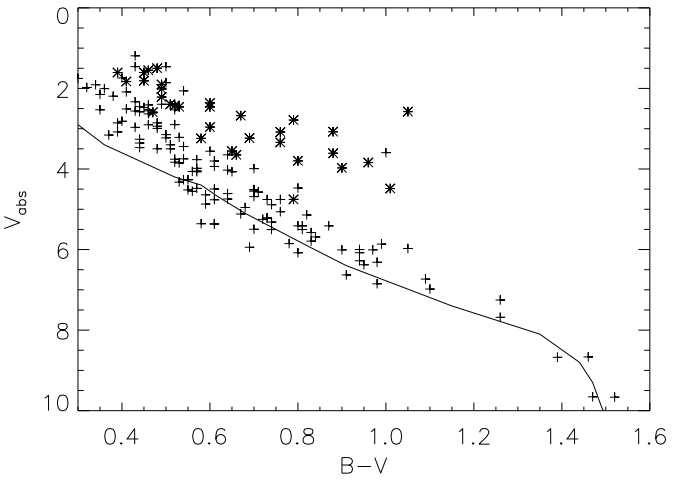

Fig. 1. Absolute V-magnitudes of the SB targets in the main sample versus their $B-V$ colors. Asterisks mark the SBs with evolved components, the solid line shows the Main Sequence from Lang (1992).

We define a sample of spectroscopic binaries (SBs) where the chance of discovering a TC is maximized. Ideally, the systems should be composed of low-mass dwarf stars because such stars are not too bright, increasing the possibility of detection of close visual companions, and have sharp lines making it easier to detect spectroscopic tertiaries. Furthermore, the stars should be nearby, leading to larger separation of tertiaries. We also want to probe the frequency of TCs to SBs with periods below and above the KCTF limit of $P \sim 7^d$, and hence consider the SBs with periods up to 30^d.

The main sample was constructed by selecting solar-type SBs from the catalog of Batten et al. (1989). No condition on the luminosity class was imposed: short orbital periods guarantee small stellar radii, hence evolved components (giants) will be excluded. It is known that luminosity classes assigned by observers are often contradictory, hence we tried to ignore them. It turned out later that some objects are in fact moderately evolved (Fig. 1).

The sample was complemented by new SBs from recent surveys of nearby stars (Latham et al. 2002; Goldberg et al. 2002; Halbwachs et al. 2003 and other). New unpublished SBs from the CORALIE ongoing survey were also

Table 1. Preliminary parameters of CORALIE binaries. The columns contain: (1) HIP number, (2) HD number, (3) orbital period, (4) semi-amplitude of the primary and (5) Notes.

HIP	HD	P_1, d	K_1, km/s	Note
2790	3277	15	5?	Uncertain SB
2848	3359	22	22.4	B-comp. to HIP 2888
19248	26354	2.5	56	$P_3 > 3000$ d
38179	64184	17.8	12.7	
45957	81044	15	8	
49161	87007	30	13.4	P_3 suspected
53217	94340	6.8	20?	Susp. $P_3 = 1200$ d
56960	101472	4.4	15.7	
73269	132173	14	31.5	
85675	158577	9.69	34.5	
94863	180445	2.5	47	SB2
97030	186160	10.7	18	
107779	207450	4.9	15.8	
114703	219175	7.1	22.9	CPM HIP 114702
116429	221818	11.6	15	

added (Table 1). A total of 200 SBs were thus selected. However, the main sample was then restricted to stars with Hipparcos parallaxes larger than 10 mas (i.e. within 100 pc). This sample contains 165 SBs with periods less than 30 days belonging to 161 stellar systems (including four multiple systems with two short-period SBs each). Each system is identified by its Hipparcos number (when several components have distinct HIP numbers, only one is retained). The main data on the sample – HIP and HD numbers, coordinates, proper motions, parallaxes, magnitudes and spectral types – are given in Table 2, available electronically. Several targets belong to the Hyades cluster.

The masses of the primary components of the SBs are either known from orbital solutions (e.g. eclipsing pairs) or estimated from the $B-V$ colors and spectral types using standard relations for the Main Sequence (MS) from Lang (1992). Despite the brightness of our targets, the task of assembling the basic data turned out to be non-trivial because the light of several components is mixed and there is a confusion between components in the catalogs. For 32 stars identified as evolved, we roughly estimated their masses $\mathcal{M}_1$ from the absolute magnitudes V_{abs} as $\mathcal{M}_1 = 0.2(9 - V_{abs})$. Those stars in Fig. 1 that are above the MS but not marked with asterisks belong to multiple systems that contain more massive evolved visual components, while the spectroscopic primaries are unevolved. The median mass of a primary in our sample is $\mathcal{M}_1 = 1.1\mathcal{M}_\odot$, the full range is 0.42 to $1.7\mathcal{M}_\odot$.

The masses of spectroscopic secondaries $\mathcal{M}_2$ are calculated from the known mass ratios in case of double-lined systems (SB2s) or from the mass functions in case of SB1s (minimum masses). It is known that minimum masses are statistically biased (Goldberg et al. 2003). However, we are not concerned with the mass ratio of SBs, so this bias does not affect the present investigation..

3. Adaptive-optics observations

Adaptive optics (AO) imaging in the near infrared (IR) is a powerful tool for discovering low-mass companions, as demonstrated by a number of recent studies (e.g. Shatsky & Tokovinin 2002). AO allows for an exploration of a large part of the parameter space that is not accessible to traditional observational techniques. This increased capacity results from the high angular resolution, high dynamic range (the ability to detect faint stars because AO concentrates light into diffraction-limited cores) and observations in the infrared which improves the contrast of low-mass companions with respect to their primary stars.

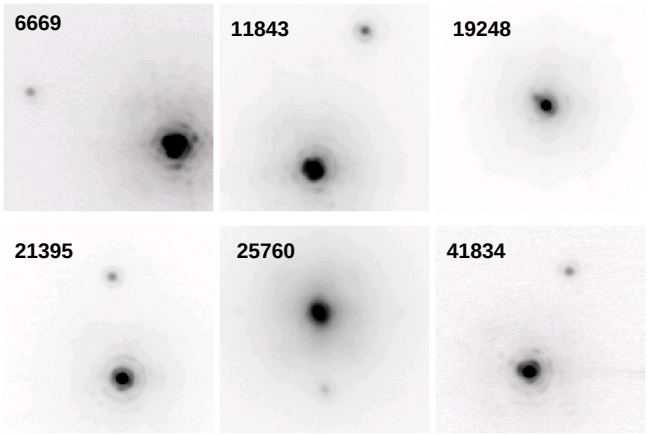

Fig. 2. Representative narrow-band NACO images of some resolved targets in $2'' \times 2''$ fields (inverted intensity scale with square-root stretch). The Hiparcos numbers are marked.

High spatial resolution images of the target stars have been obtained at the VLT telescope using the NAOS-Conica adaptive optics system, NACO[1], on November 8-9, 2004 and on July 6-12, 2005. We observed 72 targets and two astrometric calibrators (see below) in the narrow-band (NB) filter centered at the wavelength 2.12 μm, to avoid detector saturation. Five stars were also observed in the J and/or H photometric bands to estimate the colors of their companions. Only targets without known TCs (or with distant tertiaries) were observed. Of the 72 stars observed, only 62 belong to our final sample. The remaining ten SBs (HIP 5436, 25760, 34003, 35600, 41834, 50966, 87330, 87370, 110514, 112009) do not satisfy the criteria for inclusion in the study sample, but we nevertheless provide data on their companions in the electronic table.

The images were processed in a standard way. The sky background and detector bias were estimated and subtracted by median filtering a series of five frames dithered on the sky. The de-biased images were then flat-fielded and

[1] http://www.eso.org/instruments/naco

combined. The relative positions and magnitudes of wide components were determined by DAOPHOT point spread function (PSF) fitting of the main star to all sources. Measurements on individual images indicate that the random error in position is about 0.5 mas in each coordinates and the rms error in magnitude difference is around 0.02^m for components with $\Delta m < 3^m$, increasing to 5 mas and 0.05^m for $\Delta m = 5^m$.

Data on close ($< 1''$) companions were processed by an alternative technique of simultaneous fitting of binary parameters and a non-negative PSF. First, we determine the initial binary parameters in Fourier space by fitting (at high spatial frequencies above the seeing cutoff) the image Fourier transform (FT) to the FT of a PSF star convolved with the binary. This initial estimate of the binary parameters then serves to de-convolve the object FT from the binary, extracting an estimate of the true (synthetic) PSF. The synthetic PSF is radially-averaged outside the ten pixel ($0\farcs13$) radius and is used in the second, final model-fitting. In this way, it is possible to measure binary parameters independently of the PSF star. The quality of this procedure is controlled by the abscence of companion traces in the synthetic PSF before its radial averaging.

Most of the new companions are well above the detection threshold (Fig. 2). In trying to recover faint and close tertiaries that escape immediate detection, we examined all images after subtracting radially-averaged profiles. This procedure reveals asymmetric features of the PSF, often persistent in the individual (non-averaged) images. We measured the parameters of eight such tentative companions and found that their separations are all close to $0\farcs1$, with a magnitude difference of about $2^m - 3^m$. The position angles of these companions differ by 170° to 180° from the VLT parallactic angle, strongly suggesting that they are telescope-related artefacts. In the case of HIP 107095, a very good radial-velocity coverage (Fekel 1997) virtually excludes the existence of our tentative $0\farcs1$ TC, unless its orbital inclination is very low. In contrast, the new close companion to HIP 19248 is real: it does not follow the parallactic-angle dependence and is confirmed by other techniques.

Relative coordinates of the components in detector pixels were transformed to on-sky positions using observations of two known wide binaries, HIP 108797 and HIP 116737. The accuracy of this calibration is entirely determined by the known angular separation and position angle of these "calibrators". We adopted the resulting pixel scale of 13.30 ± 0.01 mas/pixel and offset of $-0.4° \pm 0.1°$ to the observed angles. The calibration remained stable between 2004 and 2005 runs. The data on newly discovered tertiaries are presented in Table 3. We also include the data on our calibrator binaries in the last rows. We thus detected 13 new TCs (as well as the known component HIP 98578B) among 62 targets from the main sample (detection rate 21%). For some new TCs, we were able to check the correspondence of their colors with those expected for the MS dwarfs (photometric confirmation), while two TCs are confirmed by proper motions. We estimate that all new companions except two are physical, and support this with statistical agruments presented in Sect. 4. Comments on selected systems are provided below.

Table 3. Data on companions discovered with NACO. The columns give (1) Hipparcos number, (2) companion identification, (3) spectral band, (4) epoch of observation, (5,6,7) measured separation, position angle and magnitude difference.

HIP	Cmp	Band	Epoch 2000+	ρ, $''$	θ, $^\circ$	Δm
6669	B	NB	4.857	1.469	69.37	5.50
		J	4.857	1.467	70.31	6.29
		H	4.857	1.466	70.04	5.84
11843	B	NB	4.857	1.422	339.2	3.55
19248	B	NB	4.857	0.104	46.11	2.61
		H	4.857	0.094	47.18	2.39
21395	B	NB	4.857	0.991	5.15	3.61
25760	B	NB	4.857	0.751	184.20	4.21
41834	B	NB	4.857	1.047	337.93	3.85
		J	4.857	1.056	336.47	4.51
	C	NB	4.857	3.573	202.83	5.30
43557	B	NB	4.857	3.446	333.73	4.28
44164	B	NB	4.857	1.851	270.83	6.93
		J	4.857	1.855	270.80	7.29
48215	B	NB	4.857	0.759	124.09	2.49
64219	B	NB	5.533	0.309	291.41	4.05
91360	Opt	NB	5.526	3.760	31.76	7.59
94863	B	NB	4.857	9.378	52.20	4.68
98578	C	NB	5.517	0.391	340.23	2.25
98578	B	NB	5.517	3.696	353.64	0.62
107779	B	NB	4.857	2.219	144.60	3.56
		J	4.857	2.226	144.59	4.16
		NB	5.522	2.233	144.30	3.45
		Calibrators				
108797	B	NB	4.857	3.848	246.37	2.52
116737	B	NB	4.857	3.890	276.96	0.98

HIP 19248 is an astrometric binary in the Hipparcos catalog. We estimate the TC period as ∼6 yr, its mass as 0.3 $\mathcal{M}_\odot$. The TC was previously inferred from CORALIE's precision RVs.

HIP 35487 has a known astrometric TC with computed orbit ($P_3 = 92$ yr, estimated separation $0\farcs4$, mass 0.34 $\mathcal{M}_\odot$) which was not detected with NACO; it must be a white dwarf.

HIP 41834 has two companions in the NACO images. However, the fainter companion C was not detected in the J-band, thus it must be an optical source.

HIP 91360 has such a faint companion that, if physical, it would have sub-stellar mass. We consider this compaion an optical source because the density of background objects near this target is very high, $N_* = 335$ (Sect. 4).

HIP 94863: a wide companion was seen by luck in the corner of a dithered field. It has been independently identified as a 2MASS photometric candidate (Sect. 4), with a consistent position. The proper motion would have moved

it by 0.″7 in 5 yrs if it were only an optical source, hence we conclude that it is physical.

HIP 98578 is a visual triple, with the new AC pair discovered here. We estimate the period of AC to be ∼100 yr; it could be detectable as astrometric perturbation in the motion of AB. The 2356-yr visual orbit computed for AB (Hopmann 1973) is premature. Without AO observations, we would wrongly consider the B component as tertiary.

HIP 107779. The new companion is confirmed as physical by our second-epoch observation and its $J-K$ color.

4. Search for companions in 2MASS

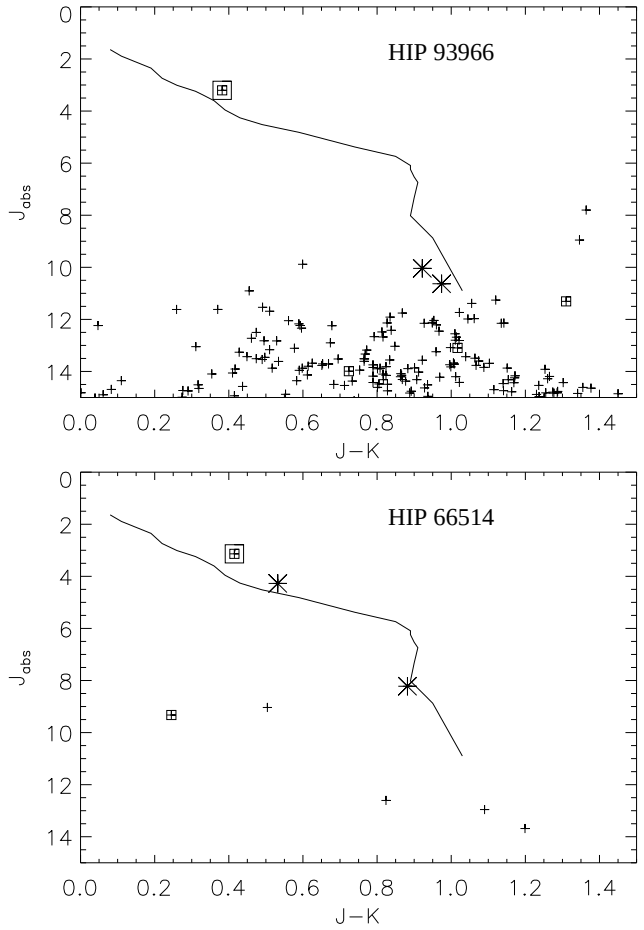

Fig. 3. CMDs for HIP 93966 in a crowded ($N_* = 187$) field (top, two optical candidates) and HIP 66514 with $N_* = 8$ and two physical companions (bottom). The primary targets are marked by large squares. The selected photometric candidates are plotted as large asterisks, remaining field stars as crosses. Stars within 30″ from the target are marked by small squares. The solid line depicts the standard Main Sequence from Lang (1992).

The SBs were examined for the presence of wide visual companions using the Two Micron All-Sky Survey (2MASS) and the Digital Sky Survey (DSS). The primary targets are bright nearby dwarfs. Many faint "companions" are found near any bright star, but the vast majority of such companions are simple line-of-sight projections or "optical" sources. However, faint *physical* companions may still hide among the multitude of optical companions. Previous generations of double-star observers were guided by statistics to separate likely physical companions from chance projections (Poveda et al. 1982). Thus, a "filter" was adopted to reject optical companions, and such a filter introduces a strong selection effect in the existing double-star catalog, WDS (Mason et al. 2001). In this study, we use the JHK_s photometry provided by 2MASS to place the companion stars on the color-magnitude diagram (CMD) and to select potential physical companions. The extinction in the J and K bands can be safely neglected for our nearby sample.

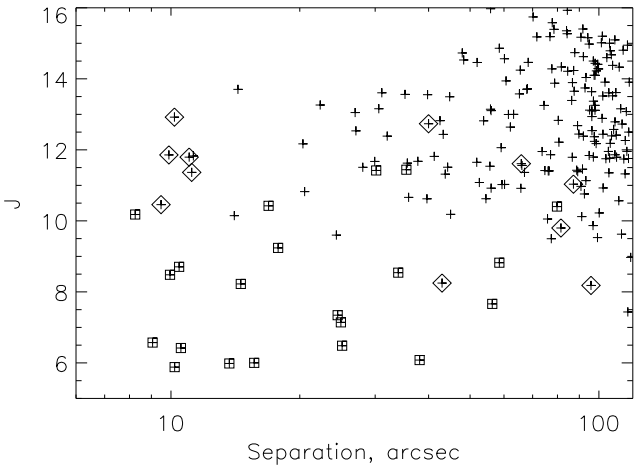

Fig. 4. Distribution of photometric candidates from 2MASS in separation ρ and magnitude J. Known physical companions are marked by squares, the new physical companions by diamonds, while crosses are likely optical (i.e. not physical) companions.

The photometry and coordinates of all stars within a 2′ radius from each of the 165 targets were retrieved from the 2MASS Point Source Catalog using the Vizier service at CDS. A total of 6079 companions were thus found. Only 202 (3.3%) were selected automatically as *photometric candidates* by their distance from the MS $\sqrt{\Delta J^2 + \Delta(J-K)^2} < 0.2^m$. We checked that this criterion selects most of the known physical companions, but it cannot be made "sharper" without the risk of losing companions. Two examples of CMDs are shown in Fig. 3. It is clear that in the fields with a large number of stars N_* the confusion impedes the detection of physical companions and that the photometric candidates in these fields are likely optical.

The statistics of photometric candidates (Fig. 4) confirms that they are mostly optical – faint and with separation ρ of the order of the field radius, 120″. In contrast, known physical companions are brighter and are distributed in $\log \rho$ almost uniformly.

In an effort to reduce the number of candidates, we discarded 36 fields with $N_* > 40$ (the median is $N_* = 13$).

Faint companions with $\rho > 60''$ and $J > 13^m$ were also discarded, as well as multiple candidates and candidates in the Hyades (HIP 20019, 20284, 20440). Excluding known physical companions, we retained 35 candidates for astrometric checking.

The targets are nearby stars with typical proper motions (PMs) of $0''.1$ per year. Physical companions must share these motions and would be displaced by $\sim 5''$ on the sky in 50 yr. Old photographic plates are over-exposed in the vicinity of the targets, hence we can check only candidates with $\rho > 20''$. The images of fields around each target were retrieved from the DSS (red Palomar plates for northern declinations and red UK Schmidt plates for southern declinations). The time base between 2MASS and DSS is around 50 yrs in the North but only around 10 yrs for southern stars.

We found photometric candidates in the DSS images and roughly measured their coordinates using the astrometric reference of the DSS, with an accuracy of about $0''.5$. When the displacement of the main target is significantly larger than $0''.5$, we can discriminate the optical companions. The majority of wide and faint companions turned out to be optical. In four cases the status of the companions remained uncertain (small PM and/or small time base), while three new companions with large separations (HIP 16042, 36328, 66514) among our 35 selected candidates were confirmed.

The distribution of new companions in the $(\log\rho, J)$ plane (Fig. 4) shows a "cluster" of 5 points near $\rho \approx 10''$. These TCs have not been checked by astrometry. However, statistical arguments show that they are all likely physical companions. We leave out HIP 94863 which lies in a crowded field ($N_* = 52$), but note that its $9''.4$ companion is physical (Sect. 3). The remaining 4 stars with such companions are HIP 3362, 17076, 20712, 60331. These targets have small stellar surface densities (N_* of 17, 13, 15, 6, average 12.75) and the companion separations are less than $11''$. Among 86 targets with $N_* < 13$, the expected number of point sources at $\rho < 11''$ is 8.7. Given that the photometric criterion selects only ≈3% of all sources, the expected number of randomly selected photometric candidates within $11''$ is 0.26; this number should be compared to the four companions actually found. In addition, there are 6 previously known *physical* TCs with similar separations of $\rho \sim 10''$.

An additional screening for new close companions has been performed by examining the 2MASS images of apparently single targets. We found such companions to HIP 43557 (confirmed with NACO) and HIP 60956. The latter is still considered as tentative.

Summarizing the results for 2MASS candidates, Table 4 lists the data on 23 known, 7 new certain, and 5 new tentative (marked with ?) companions – a total of 35 TCs. The known companions are marked "MSC". We see that existing catalogs contain about 2/3 of the wide TCs; another 1/3 are added in this work.

Table 4. Tertiary companions found in 2MASS. The columns give (1) HIP number, (2,3) separation and position angle, (4) J magnitude of the companion, (5) $J-K$ color, (6) status, with MSC for previously known companions.

HIP	$\rho,''$	$\theta,^\circ$	J	$J-K$	Status
3362	11.18	278.13	11.366	0.801	new
7874	10.45	31.34	8.705	0.749	MSC
12189	38.11	274.44	6.080	0.258	MSC
16042	95.82	129.08	8.182	0.556	new,CPM
17076	9.89	245.34	11.857	0.839	new
20712	11.03	119.67	11.795	0.861	new
24663	9.95	148.60	8.481	0.460	MSC
31850	30.17	248.74	11.420	0.840	MSC
36238	43.00	323.59	8.249	0.780	new,CPM
41211	35.49	328.69	11.441	0.841	new?
42172	10.20	25.11	5.882	0.385	MSC
45957	8.25	118.02	10.179	0.787	MSC
47053	24.95	149.20	7.142	0.271	MSC
52064	3.67	342.14	6.136	0.034	MSC
56809	9.06	248.40	6.573	0.615	MSC
56960	79.81	334.28	10.403	0.705	MSC
60331	10.19	320.43	12.921	0.896	new
60956	5:	355:	-	-	new?
61910	58.52	228.80	8.822	0.444	MSC
66514	56.34	258.63	7.662	0.532	MSC
66514	65.86	254.25	11.610	0.882	new,CPM
73269	81.52	39.64	9.800	0.716	new?
74037	17.80	19.75	9.239	0.494	MSC
84586	33.97	92.78	8.542	0.913	MSC
91009	16.91	45.50	10.424	0.902	MSC
94863	9.48	53.03	10.457	0.769	NACO
98578	3.00	353.70	6.251	0.103	MSC
103569	10.55	67.95	6.419	0.283	MSC
104026	39.99	201.07	12.735	0.865	new?
107354	14.56	289.05	8.224	0.572	MSC
108461	13.69	246.71	5.984	0.379	MSC
111802	24.52	350.36	7.344	0.853	MSC
114379	15.65	75.94	6.002	0.332	MSC
114639	87.20	205.54	11.033	0.805	new?
114703	25.12	355.67	6.484	0.338	MSC

5. Parameters of tertiary companions

Table 5 contains the data on previously known companions to the SBs which have been extracted from the MSC (Tokovinin 1997) and combined with the new detections in a single database. Additional bibliographic searches for stars without reported tertiaries have been made through SIMBAD. We also scanned the fourth catalog of interferometric measurements (Hartkopf et al. 2004 – INT4) and marked the stars that were observed by speckle interferometry. Also, the ninth catalog of spectroscopic binary orbits (Pourbaix et al. 2004 – SB9) was searched for new orbits.

A part of Table 5 with the information on all known components is printed here; the full Table is available electronically. Below we describe the information in this Table.

Table 5. Data on companions (fragment). The columns are explained in the text.

HIP	ID	Type	Separation		Period		$\mathcal{M}_1$	$\mathcal{M}_2$	Remark
47053	Aa,Ab,A	S2	0.471	mas	1.681	d	1.54 a	1.46 a	SB 575
47053	A,C,AC	v	0.300	”	64.257	y	3.00 s	0.98 a	COU 2084
47053	AC,B,*	Chrp	25.000	”	41.099	ky	3.98 s	1.65 s	STF 1369
47053	Ba,Bb,B	S1	2.530	mas	28.231	d	1.29 a	0.36 m	1998AstL...24..288T
48215	Aa,Ab,A	S1	0.924	mas	3.390	d	1.11 a	0.29 m	SB 584 DI Leo
48215	A,B,*	AO	0.759	”	130.282	y	1.40 s	0.61 v	NACO-2004
48273	Aa,Ab,*	S2	1.196	mas	3.055	d	1.21 a	1.15 q	SB 585
48833	Aa,Ab,*	S2	1.057	mas	3.055	d	1.26 a	1.20 q	SB 584
49018	Aa,Ab,A	E,S2	0.690	mas	1.070	d	0.78 a	0.53 q	DH Leo, SB 591
49018	A,B,*	v	0.220	”	14.190	y	1.31 s	0.50 v	CHARA 145
49161	Aa,Ab,*	S1	3.965	mas	30.000	d	0.74 a	0.50 q	CORALIE
49809	Aa,Ab,*	S1	5.557	mas	28.098	d	1.49 a	0.20 m	SB 601

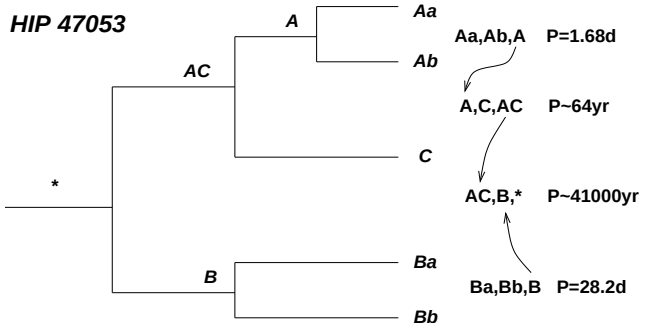

Fig. 5. Example of the hierarchical quintuple system HIP 47053 and the identifications of its sub-systems (see text).

Additional comments on specific systems are provided in the electronic notes to Table 5.

Identification of each system is given in the column 2 as a sequence of 3 designations (primary, secondary, parent) separated by commas. These codes describe the hierarchy of each system by referencing to the parent, as illustrated in Fig. 5. The system at the highest hierarchy level (root) is coded with an asterisk, it is the parent of the wide subsystem AC,B in Fig. 5.

The type code of each system shows the method(s) of its discovery, in the same manner as in the MSC. For example, **S1** and **S2** refer to single- and double-lined SBs, **E** to eclipsing systems, **C** stands for wide (CPM) systems (the following small letters describe which criteria of physical relation between components are satisfied, see MSC and notes to the electronic Table 5), **v** means a resolved system closer than 3″, **V** stands for a visual binary with computed orbit, etc. Two new special types are **AO** (companions discovered with NACO) and **2M** (2MASS companions).

The separation between components is given together with units (arcseconds or milliarcseconds). For systems with known orbits the separation refers to semi-major axis, otherwise it is the observed separation ρ. The separation of SBs is estimated from known periods and Kepler's Third Law as

$$\rho \approx pP^{2/3}\mathcal{M}^{1/3}, \quad (1)$$

where p is the parallax (arcseconds), P is the orbital period in years and the system mass $\mathcal{M}$ is in solar units. Here we assume implicitly that separation is statistically equivalent to semi-major axis.

Periods are given in the next column, in units of days, years or kiloyears. For wide systems without computed orbits the periods are estimated from ρ with Eq. 1.

Masses of primary and secondary components $\mathcal{M}_1$ and $\mathcal{M}_2$ are given in solar mass units with codes indicating the method of mass estimation. The preferred methods are **a** – from spectral type (cf. Sect. 2) or ***** – estimated by other authors from orbit solutions or detailed models. Other codes are **l** – evolved components, **s** – sum of sub-components' masses, **q** – SB2 secondary, **m** – minimum mass of SB1 secondary, **v** – mass from magnitude difference, **:** – unknown magnitude difference, **?** – uncertain companions. Masses of all new components (AO and 2M types) were estimated from the magnitude differences in the K band using the relations of Henry & McCarthy (1993) and taking into account the light of the spectroscopic secondary.

Remarks provide common identifications for the subsystems, e.g. the SB numbers in Batten et al. (1989) catalog, visual double-star designations, bibcodes, etc.

The sample contains 165 spectroscopic binaries belonging to 161 stellar systems; 79 have no known tertiaries, and the remaining 86 SBs have one or more companions (64 triples, 11 quadruples, seven quintuples – a total of 82 systems). Of these, six TCs are uncertain (our 2MASS detections, doubtful speckle companions, etc.), but they are still considered in the statistics. The fraction of SBs with TCs should be no less than 86/165=0.52. Not all TCs have been discovered yet. Known distant companions are considered as tertiaries, but in some systems the true tertiaries at closer separations are not known and the present "tertiaries" are actually higher-level companions, as turned out to be the case for HIP 98578, where a new, closer companion to SB was discovered with NACO in addition to the known wide companion.

Mass ratios of TCs are defined here as $q_3 = \mathcal{M}_3/\mathcal{M}_1$, i.e. relative to the spectroscopic primary, not to the total mass of the SB. There is no ambiguity for triples, but for systems with more components, as in Fig. 5, the choice of tertiary is not always evident. We select $\mathcal{M}_3$ to be the largest mass of all components at the next higher level of hierarchy. Thus, the binary Ba,Bb in Fig. 5 has Aa as its most massive tertiary, $q_3 = 1.10/1.29 = 0.85$, $P_3 \approx 41000$ yr. However, another close binary Aa,Ab in the same system has a tertiary component C, hence $q_3 = 0.98/1.10 = 0.89$, $P_3 \approx 64$ y.

6. Detection limits

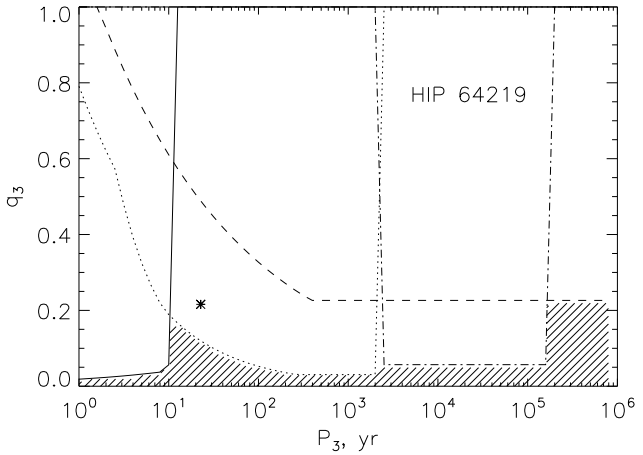

Fig. 6. Estimated limits of companion detection by different techniques for HIP 64219. Full line – radial velocities, dotted line – NACO, dashed line – visual and CPM, dash-dotted line – 2MASS. The NACO companion is marked by asterisk. The overall probability of TC detection for this object is zero in the hatched zone below all curves and one above.

For any given star and any observing technique, the probability of detecting a TC depends on the companion's parameters – its period, P_3, and its mass ratio, q_3. This probability should be a smooth function of the parameters, but we simplify it here as a sharp limit, assuming that all TCs with $q_3 > q_{\rm lim}(P_3)$ are detected and less massive companions are not. An example of such limits for one target is shown in Fig. 6. By averaging the detection probabilities for the whole sample, we again obtain a smooth detection probability (Fig. 7). The method of computing detection limits is detailed in Appendix A for each observing technique. We specify the detection limits for each *system*, hence the four systems with two SBs each have only one entry per system. However, these systems are at least quadruple and pose no problem in the statistics.

Detection limits were converted into estimates of the minimum observable mass ratio q_3 (Sect. 5) and compared to the actual mass ratios of known and new TCs in Fig. 8.

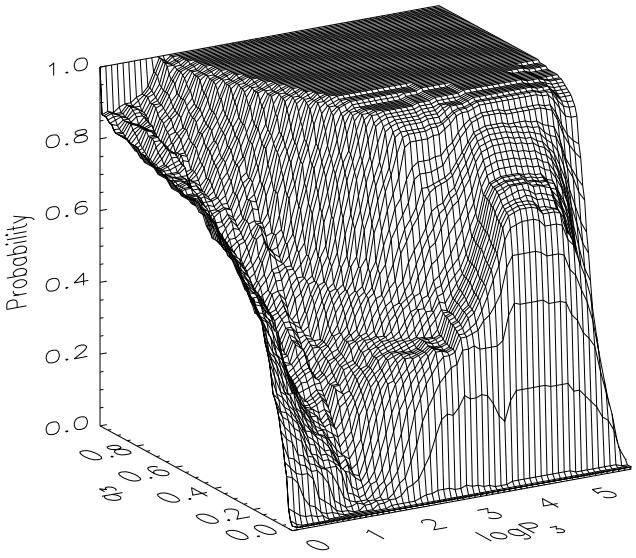

Fig. 7. Probability of tertiary companion detection for the whole sample as a function of $\log P_3$ and q_3.

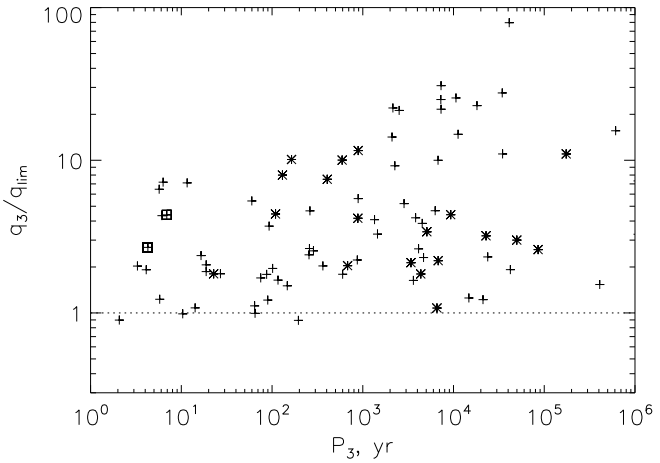

Fig. 8. Comparison of the actual mass ratios of tertiary components q_3 with their estimated detection limit q_{lim}. Known TCs are plotted as pluses, the new (NACO and 2MASS) TCs as asterisks. Uncertain TCs are marked with squares.

We see that only several tertiaries are slightly below the estimated detection limit and conclude that the limits can be used confidently in the statistical analysis.

7. Statistics of tertiary companions

7.1. Mass ratios and periods of tertiaries

Figure 9 shows the distribution of TCs in (P_3, q_3) space. Known companions at higher hierarchical levels (like the component Ba relative to the Aa, Ab system in Fig. 5) are also plotted as squares for comparison. The curves indicate detection limits. As expected, new TCs detected in this work mostly have low mass ratios.

We note that 16 tertiaries ($17 \pm 4\%$) have $q_3 > 1$, i.e. the spectroscopic primary is not the most massive compo-

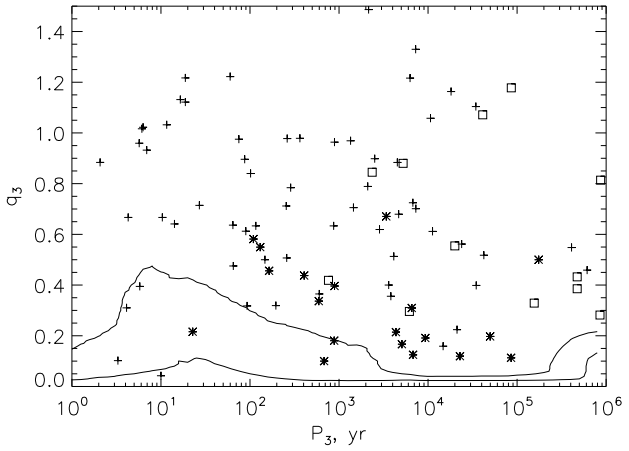

Fig. 9. Mass ratio of tertiary to spectroscopic primary as a function of tertiary orbital period. The known components are plotted as pluses, the new components as asterisks. The squares denote components at the next hierarchical level, not considered in the main statistical analysis. The lines trace detection probabilities of 10% (lower) and 50%(upper), i.e. the contours of the surface in Fig. 7.

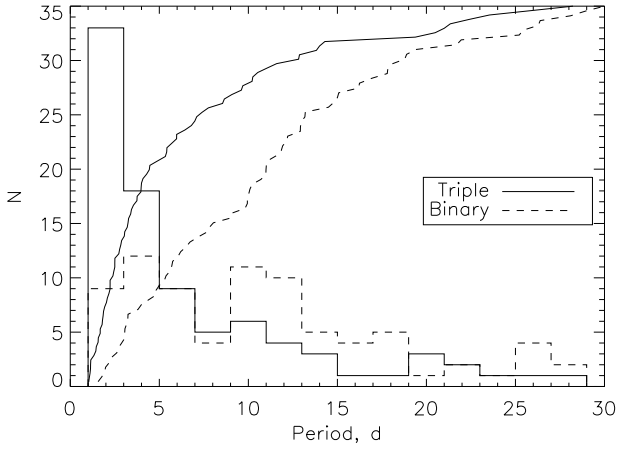

Fig. 10. Histograms and cumulative distributions of orbital periods of spectroscopic binaries with tertiaries (Triple, full line) and without tertiaries (Binary, dashed line). The larger fraction of short periods among those SBs which belong to triples is evident.

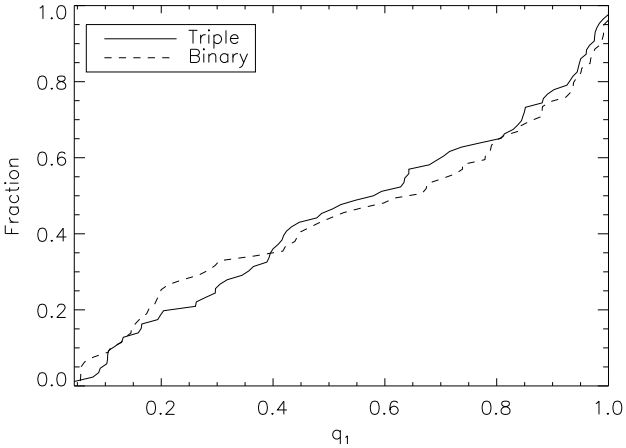

Fig. 11. Cumulative distributions of the mass ratios of spectroscopic binaries with tertiaries (Triple, full line) and without tertiaries (Binary, dashed line).

nent in the system. If components were selected randomly, one would expect this fraction to be 1/3 or higher (in systems with more than 3 components we select the most massive tertiary). Hence, we confirm the known tendency that the most massive components in multiple systems are preferentially found in close sub-systems.

Interestingly, we find only three TCs with $P_3 > 10^5$ yrs, but also six higher-level companions wich such long periods. Thus, a decrease of the number of TCs at long periods must be real, not a selection effect.

7.2. SBs with and without tertiary companions

The cumulative distributions of the orbital periods of SBs with and without TCs are compared in Fig. 10. It is evident that SBs within multiple systems have, generally, shorter orbital periods. The maximum difference between the cumulative distributions normalized to 1 reaches 0.30. The numbers of objects in the histograms are 86 and 79, so the Kolmogorov-Smirnov test rejects the hypothesis that both distributions are equal with a significance level of 0.999. Some of the SBs considered today as "single" have yet undiscovered tertiaries (e.g. suspected astrometric companions), so the actual difference between the distributions is likely to be larger. The presence of a TC shortens the period of a spectroscopic binary. On the other hand, the existence of such difference shows that SBs without TCs (pure binaries) do exist.

In contrast, there is no difference in the mass ratio distributions of the SBs with and without TCs: both show a slight excess of systems with nearly equal-mass components (twins), but otherwise the distributions are almost uniform (Fig. 11). As noted in Sect. 2, the mass ratios of SB1 are biased, but this bias is independent of the presence of the TC.

7.3. Period-period diagram

There seems to be no correlation between the SB orbital periods P_1 and the TC periods P_3 (Fig. 12, asterisks). However, the shortest TC periods (lower boundary of points) seem to increase with P_1. For comparison, we overplot nearby solar-type multiples from the MSC (crosses, cf. Tokovinin 2004). Multiple systems with wide inner binaries are almost exclusively found with period ratios P_3/P_1 of between 5 and 10 000. In contrast, our multiples are *all* quite far from the dynamical stability limit and can have period ratios $> 10^4$. This difference may be understood if the SBs were formed with longer periods and later migrated to shorter periods. The relative

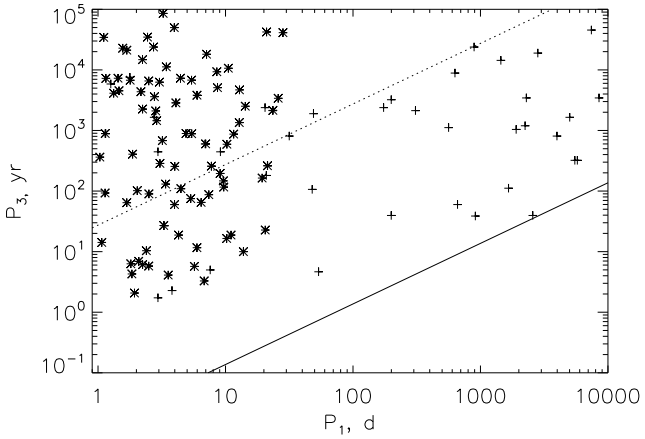

Fig. 12. Comparison of the SB periods (horizontal axis) with respective tertiary periods (vertical axis). The full line denotes the dynamical stability limit $P_3 = 5P_1$, the dotted line marks the period ratio of 10 000. Our sample is plotted as asterisks, other triple systems from MSC are plotted as crosses.

paucity of inner sub-systems with periods of a few months matches this scenario, although it could probably also be explained by observational selection. The lowest observed $P_3 \sim 2$ yr implies that the progenitors of these SBs had $P_1 \leq P_3/5 \sim 150^d$, otherwise those systems would have disintegrated through dynamical instability (e.g. Mardling & Aarseth 2001).

7.4. Companion distribution by Maximum Likelihood

.

An estimate of the TC distribution over period P_3 is derived here by the Maximum Likelihood (ML) method. The parameter space is divided into bins, the fraction of TCs in each bin is $\mathbf{f} = \{f_k\}$. The probability of obtaining the actual data $\mathcal{L}$ is called the likelihood. By minimizing its natural logarithm S

$$S(\mathbf{f}) = -2 \ln \mathcal{L}(\mathbf{f}), \quad (2)$$

we find the estimate of $\mathbf{f}$. Moreover, the ML method permits us to determine confidence intervals of the estimated parameters or their functions (Avni et al. 1980). Mathematical details and ML equations are given in Appendix B.

In the analysis, we select five bins for P_3 uniformly covering the $\log P_3$ space from one to 10^6 yrs. The detection probabilities are computed as a surface above the $q_{\rm lim}(P_3)$ curve in each period bin. This is strictly true only for a uniform distribution of q_3. The actual q_3 distribution does in fact appear rather uniform (Fig. 9). A more correct analysis of the joint TC distribution in P_3, q_3 (with 3 bins in q_3) has been performed and gives practically identical results.

The total TC fraction estimated by ML, i.e. corrected for incompleteness, is $63 \pm 5\%$. Considering the difference between short- and long-period SBs, we split our sample in two roughly equal parts: close ($P_1 < 7$ d, 90 systems) and wide ($P_1 > 7$ d, 75 systems), and repeat the ML analysis for these sub-samples. The results are shown in Table 6 and in Fig. 13. The errors of the TC frequency are determined by the shape of the S-function near its minimum, as illustrated in Fig. B.1. We also provide in Table 6 the raw (uncorrected) TC frequencies $f_{\rm raw}$ to show that our correction for incompleteness is not dramatic. The calculation was repeated ignoring uncertain TCs, and only a slight reduction of the estimated TC frequency results.

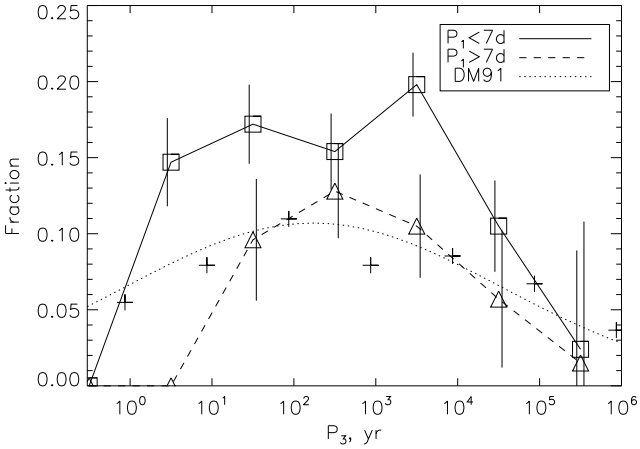

Fig. 13. Period distributions of TCs around close SBs (squares) and wide SBs (triangles). The error bars correspond to $\pm 1\sigma$. The distribution of solar-type binaries from DM91 is plotted for comparison (dotted line and crosses).

Table 6. Frequency of tertiary companions in two subsamples. N is the number of systems in each sample, $f_{\rm raw}$ is the TC frequency uncorrected for incomplete detections, f is the TC frequency estimated by the ML method. The numbers in italics are obtained by discarding uncertain companions.

Sample	N	$f_{\rm raw}$	f
$P_1 < 7$d	90	0.66	0.80 ± 0.06
	88	*0.65*	*0.79 ± 0.06*
$P_1 > 7$d	75	0.33	0.40 ± 0.06
	71	*0.30*	*0.36 ± 0.06*
All	165	0.52	0.63 ± 0.05

The sample was then further sub-divided into four groups ranked over SB periods, and the calculation of the TC frequency was done for each group separately (Fig. 14). For the shortest periods, $P_1 < 2.9^d$, the estimated TC frequency is as high as 96%.

It is clear that many SBs have tertiary companions. But companions are typical also for normal solar-type field stars (Duquennoy & Mayor 1991). Is there any difference between SBs and field stars with respect to wide compan-

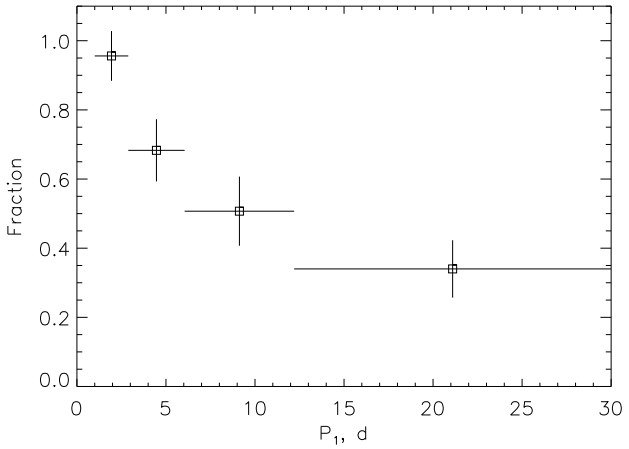

Fig. 14. Frequency of tertiary companions as a function of SB period.

ions? We compare in Fig. 13 the companion frequencies in these samples, both corrected for selection effects. Overall, the companion frequency in the DM91 sample for periods above one yr is 50% – higher than in the wide-SB subsample. On the other hand, the fraction of companions to close SBs is clearly increased. Their periods range from a few years to several thousand years.

7.5. High multiplicities

Our sample contains 64 triples and many systems of multiplicity higher than 3: 11 quadruples and seven quintuples (Sect. 5). Batten (1973) introduced f_n – the fraction of systems of multiplicity n and higher to systems of multiplicity $n-1$. For our sample, $f_4 = (11+7)/64 = 28\%$ and $f_5 = 7/11 = 64\%$. These numbers are comparable to the high-multiplicity frequencies in the MSC: $f_4 = 179/626 = 29\%$ and $f_5 = 38/141 = 27\%$ (Table 1 of Tokovinin 2001). Spectroscopic binaries from the MSC, such as HIP 76563/76566 (two SBs of 3.27^d and 14.28^d in a system with six components), are not included in the sample. This is done to avoid intentional bias towards high multiplicity.

8. Summary

1. The period distributions of SBs with and without tertiary companions (TCs) are significantly different. This proves the existence of pure SBs without TCs.
2. The mass ratio distributions of SBs with and without TCs are identical.
3. The frequency of TCs is 63% for the whole SB sample. However, it is a strong function of the SB period, reaching 96% for the close ($P_1 < 3^d$) SBs and decreasing to 34% for SBs with $P_1 > 12^d$ (Fig. 14). The last number is less than the companion frequency of ∼50% for G-dwarfs in the field. These results are robust because the TC detection does not depend on the SB period.
4. The periods of most TCs in our sample range from 2 yr to 10^5 yr. There is no correlation between P_3 and P_1. The triple systems with $P_1 < 30^d$ have large period ratios and are very stable dynamically (Fig. 12).
5. The TCs are more massive than spectroscopic primaries in a small fraction (17% ± 4%) of multiple systems, suggesting that there is a tendency of the most massive component to be found preferentially in shortest-period sub-systems.

9. Discussion

It seems that the properties of close SBs are established early in their evolution. In a compilation of pre-Main Sequence (PMS) SBs by Melo et al. (2001), the period distribution is not different in any significant way from the distribution in our sample. For example, SB periods are divided almost equally between $1^d - 7^d$ and $7^d - 30^d$ intervals. The observed frequency of TCs in the Melo et al. PMS sample, 42% ± 19% (Sterzik el at. 2004), is not different from the *observed* TC frequency of 52% in our sample of SBs in the field.

Our main result (Fig. 14) shows that essentially all very close SBs are members of higher-order systems. The KCTF mechanism is most likely responsible for shortening SB periods during their life on the Main Sequence. It acts independently of the TC period and mass: even a very wide and low-mass companion can influence the SB, given sufficient time. The period of Kozai cycles is of the order of $P_3(P_3/P_1) \sim 10^6$ yr for a typical tertiary period of $P_3 = 1000$ yr and the period of an SB progenitor of $P_1 = 1$ yr. It takes many ($> 10^2$) cycles to complete the KCTF evolution, hence it could not occur at the PMS stage. The formation of very close PMS SBs is not possible because the PMS stellar radii are too large and a contact PMS binary would rapidly merge (Whelan 1970).

For SB periods longer than 3 days, we find an increasing proportion of pure SBs without tertiaries. The existence of non-triple SBs is clearly demonstrated by this study. We see that the frequency of wide TCs to binaries with $P_1 > 12^d$ is *lower* than the companion frequency to single solar-type stars. These pure SBs have not passed through KCTF evolution. What, then, was the mechanism which produced their orbital decay?

Sterzik, Durisen & Zinnecker (2004) discuss various processes of binary formation in a systematic way and provide suitable scaling laws. Molecular cores fragment into mini-clusters of the size of order 100 AU. The system crossing time turns out to be shorter than the accretion time scale, hence stars build their masses and interact dynamically simultaneously. An accreting multiple system becomes tighter (Umbreit et al. 2005). Close approaches of the components of an unstable multiple system lead to ejections and formation of a close binary with a semi-major axis ∼ 10 times shorter than the system size. Joint action of accretion and disruption can thus produce close SBs without additional companions. To form a 10^d SB

(semi-major axis 0.1 AU), we need a typical precursor multiple system of ∼1 AU size.

Not all primordial multiples are unstable. If orbits of distant companions contain the bulk of a system's angular momentum (as should often be the case), there are no close approaches causing disintegration. The hardening of inner orbits in such systems can be primarily driven by accretion and interactions with a disk. An interesting alternative has been suggested by Namouni (2005): an orbit can become eccentric if the system moves with acceleration, e.g. caused by an asymmetric jet or a TC, and then tidal forces will produce a close SB in analogy to the KCTF process.

Some stable TCs will be lost at later stages by dynamical interaction with other members or systems of a primordial star cluster (Kroupa 2001), again leaving pure SBs.

Accretion on a close binary biases its mass ratio towards 1. Indeed, the mass-ratio distribution of SBs is nearly uniform (Goldberg et al. 2003). SBs with equal-mass components (twins) can be explained this way (Tokovinin 2000; Bate & Bonnell 1997). It is remarkable that the mass ratio distributions of SBs with and without TCs are the same (Fig. 11), pointing to a common process of their mass buildup. A general tendency to find the most massive component of a multiple system as a primary in the SB is confirmed here. It can be explained both by accretion physics and by pure N-body dynamics. However, we find that distant TCs have often comparable masses or are even more massive than the SB (Fig. 9), contradicting the simulations of Delgado-Donate et al. (2003) who predict *only* low-mass TCs.

It becomes thus increasingly clear that close binaries were formed by a combination of different processes (some probably not yet identified) and that their orbits and multiplicity were further modified by subsequent evolutionary effects such as KCTF. How efficient is the KCTF mechanism in producing close SBs? Case-by-case modeling (Kisseleva et al. 1998) should now be complemented by a statistical analysis. Additional information on the KCTF will be obtained from the relative orientation of orbits in close triple systems which are now observable with long-baseline interferometry (e.g. Muterspraugh et al. 2005).

This work can be considered as a small step towards complete multiplicity statistics in the solar neighborhood, still largely unknown because of strong observational selection effects. For example, is the paucity of $\sim 100^d$ inner periods in multiple stars (Fig. 12) real? Is it a fossil record of inner-orbit decay? A systematic census of *all* companions in nearby solar-type stars using a combination of observing techniques is required to answer these questions.

Acknowledgements. We thank the staff of the Paranal observatory (and especially N. Ageorges) for efficient execution of our program. The comments of the Referee, H. Zinnecker, helped to improve the article. We are grateful to R. Blum for language editing of the manuscript. The SIMBAD database maintained by the University of Strasbourg has been consulted extensively. This work makes use of data products from the Two Micron All Sky Survey and Digital Sky Survey.

Appendix A: Discussion of detection limits

The knowledge of the detection limits of various observing techniques is essential to characterize the completeness of the TC statistics (Sect. 6) and to correct the final results (Sect. 7.4). The limits of each technique are discussed and modeled below.

A.1. Adaptive optics

We studied the detection limits for triple companions in our NACO observations of spectroscopic binaries. At each radial distance from the spatially unresolved SB the rms fluctuation σ in the flux over the corresponding circle was computed, and the detection limit was assumed to be 5σ. This procedure has been checked by simulating artificial companions and then detecting them visually. The resulting detection limit is described by a model

$$\begin{aligned} \Delta K &\leq \quad 7r, \qquad \rho \leq 0\farcs1 \\ \Delta K &\leq 5r + 0.9, \quad 0\farcs1 < \rho < 1\farcs5 \\ \Delta K &\leq \quad 9.05, \qquad \rho \geq 1\farcs5, \end{aligned} \tag{A.1}$$

where $r = \log(\rho/0\farcs035)$. The diffraction limit at $\lambda = 2.12$ μm is $\lambda/D = 0\farcs054$. A similar model was used by Shatsky & Tokovinin (2002). Our NACO detection limits are corroborated by Brandeker (2004, his Fig. 4).

A.2. Visual and CPM companions

The detectable magnitude differences of known visual companions increases with their separation ρ. The upper envelope corresponds to

$$\Delta V \;\leq\; 4.5\log(\rho/0\farcs05). \tag{A.2}$$

The components lying at this limit were all discovered with speckle interferometry (cf. INT4). Thus, (A.2) may be somewhat optimistic for 1/2 of our systems that have never been observed with speckle techniques according to INT4. No new companions are given in the CHARM catalog of lunar occultaions and long-baseline interferometry by Richichi et al. (2004). An additional constraint that the apparent magnitude of a companion should be brighter than $V = 15^m$ is introduced because fainter stars are generally not detected as common-proper-motion (CPM) companions.

A.3. Radial velocities

A TC modulates the center-of-mass velocity of the SB with a longer period. The probability of detecting such modulation depends on the precision of radial-velocity

observations σ, their number N and the time span ΔT. Studies of detection limits with simulations (Halbwachs et al. 2003) established that the relevant parameter is the radial velocity amplitude A_0 of a circular-orbit binary with the same period and 90° inclination,

$$A_0 = \frac{213 \mathcal{M}_3 P_3^{-1/3}}{\mathcal{M}^{2/3}}, \quad \text{(A.3)}$$

where A_0 is in km/s, tertiary mass $\mathcal{M}_3$ and the SB system mass $\mathcal{M}$ are in solar masses, and the tertiary's period P_3 is in days. Following Halbwachs et al., we model the spectroscopic detection limit conservatively as $A_0/\sigma > 3$ for all periods shorter than the data span ΔT, and as $A_0/\sigma > 3 + 20\log(P_3/\Delta T)$ for periods shorter than $2\Delta T$. The actual detection limit may extend to periods P_3 much longer than ΔT if the data are analyzed carefully, but we prefer to be conservative here by assuming the sharp loss of detection capacity at $P_3 > 2\Delta T$.

For each SB, we determined the relevant parameters σ and ΔT either from the data given in SB9 (Pourbaix et al. 2004) or from the original publications. The quality of spectroscopic orbits varies greatly, from crude orbital solutions made some 80 years ago (e.g. HIP 5689, 72524, 86263) to high-precision velocities (HIP 80686) or long-term coverage (HIP 107095). Moreover, orbits are often computed by combining radial velocities of different quality or with different systematic offsets. Thus, any model of spectroscopic detection limit is necessarily very crude and A_0/σ is only an indicative parameter, at best.

Despite uncertainties in the spectroscopic detection limits, we note that half of our sample has $\Delta T > 5.5$ yr, for 78% of SBs $\Delta T > 2$ yr. The median error is $\sigma = 1$ km/s. The TCs with periods of a few years would have a good chance of being discovered spectroscopically, hence the paucity of such companions in our sample must be real.

A.4. Astrometry

Astrometry is a poweful technique to detect low-mass companions with orbital periods over several years. Makarov & Kaplan (2005) recently published a catalog of astrometric binaries revealed either by a significant difference between "instantaneous" proper motion (PM) measured by Hipparcos and long-term PM in the Tycho-2 catalog ($\Delta\mu$ binaries) or by the acceleration measured directly by Hipparcos ($\dot{\mu}$ binaries, also known as G-solutions in Hipparcos). There are 11 astrometric binaries in common with our sample, of which six are already listed here with TCs discovered by other techniques (including HIP 19248 and 64219 resolved for the first time here). We did not resolve two $\dot{\mu}$ binaries, HIP 35487 and 114639, with NACO, possibly because their astrometric companions are white dwarfs (cf. discussion in Notes to Table 5).

Gontcharov et al. (2001) published a similar study: they brought historical astrometric catalogs into the Hipparcos system and identified several stars as astrometric binaries. However, only a few astrometric orbits of these stars are published to date (none for our sample), and Makarov & Kaplan (2005) did not independently confirm the PM variations of many stars. We observed with NACO but did not resolve HIP 67153, 80686, 85365, 86263 listed as binaries by Gontcharov et al. Here we consider astrometric detections without published orbits only as hints of the existence of TCs. Hence we do not take into account astrometric companions in our statistics.

Appendix B: Maximum Likelihood method

Problem layout. Suppose that a total of N targets have been surveyed. We determine the distribution of companions over parameters by dividing the parameter space into K bins, the fractions of companions in each bin are denoted as $\mathbf{f} = \{f_k\}$. Let $N_{i,k}$ be the number of detected companions for i-th star and k-th bin (1 when a companion is detected, 0 otherwise). The total number of companions per bin is $N_k = \sum_i N_{ik}$. Thus, a raw estimate of companion frequency will be

$$f_{k,\mathrm{raw}} = N_k/N. \quad \text{(B.1)}$$

In fact the probabilities of companion detection for each star and each bin $d_{i,k}$ are generally less than 1, so we have to account for incomplete detections. This is best done by the Maximum Likelihood (ML) technique. First, we evaluate the probabilities of observations for each star p_i and compute the *likelihood function*

$$\mathcal{L} = \prod_i p_i(\mathbf{f}). \quad \text{(B.2)}$$

By minimizing the natural logarithm $S = -2\ln\mathcal{L}$ over parameters $\mathbf{f}$ we estimate the parameters. The contours of S in the $\mathbf{f}$-space define confidence limits of the parameter estimates: $\Delta S = 1$ corresponds to the 68% interval ("1σ"), $\Delta S = 2.71$ to 90% and $\Delta S = 4$ to 95%, in direct analogy with the Gaussian probability distribution (Avni et al. 1980).

Independent detections. In the simplest case we assume companion detections in each bin to be independent of other bins. The average expected number of detected companions is $f_k d_{i,k}$, and the probabilities are computed from the Poisson distribution,

$$p_i = \frac{(f_k d_{i,k})^{N_{i,k}}}{N_{i,k}!} \exp\left(-f_k d_{i,k}\right). \quad \text{(B.3)}$$

Considering that $N_{i,k}$ only takes values of 0 or 1, the likelihood equation can be written as

$$-2\ln\mathcal{L} = -2\sum_{i=1}^{N}\sum_{k=1}^{K}[N_{i,k}\ln(f_k d_{i,k}) - f_k d_{i,k}] + \text{const.} \quad \text{(B.4)}$$

By differentiating (B.4) over f_k we obtain the estimates

$$\hat{f}_k = \frac{N_k}{\sum_i d_{i,k}}. \quad \text{(B.5)}$$

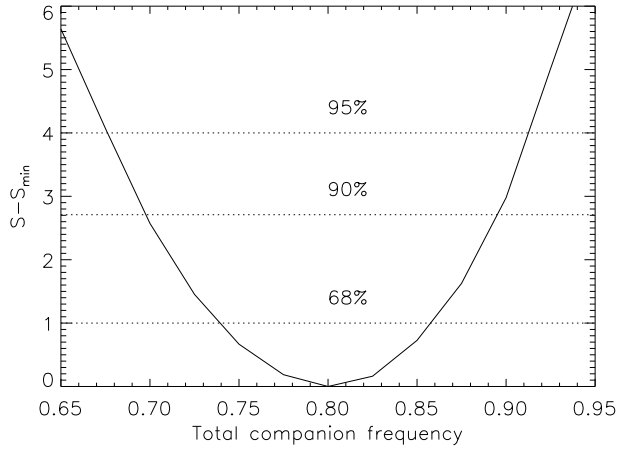

Fig. B.1. The shape of the $S-S_{min}$ function near its minimum and the confidence intervals on the total companion frequency for a sub-sample of close SBs, $P_1 < 7$d.

This result is intuitive: we simply correct the observed companion frequencies $f_{\rm raw}$ by the average probabilities of detection $\sum_i d_{i,k}/N$.

We compute the probabilities $d_{i,k}$ as fractional surfaces of each bin above the detection limit curve $q_{\rm lim}(P_3)$, individually for each star. The underlying assumption is that the (unknown) companion distribution within each bin is uniform. Looking at Fig. 9, we note that there are no strong gradients of companion frequency over q_3 or P_3, hence the assumption is good.

Mutually exclusive detections. A given spectroscopic binary can have no more than one tertiary companion, by definition. Thus, a detection of a companion in some bin automatically excludes companions in other bins. Denoting by f_0 the probability of no companions, we have an additional condition $\sum_k f_k + f_0 = 1$.

According to the Bayes theorem, the probability of obtaining an observational result for the i-th star is related to the distribution f_k and the conditional probabilities (detecting or not detecting companion) $p(i|k)$,

$$p_i = \sum_{k=0} p(i|k) f_k. \tag{B.6}$$

In the case of companion non-detection, the probability p_i^- is

$$p_i^- = f_0 + \sum_{k=1} (1 - d_{i,k}) f_k = 1 - \sum_{k=1} d_{i,k} f_k, \tag{B.7}$$

while for stars with companions the probabilities are simply $p_i^+ = f_k d_{i,k}$, according to (B.3). This leads to the likelihood function

$$\begin{aligned} -2\ln\mathcal{L} \;=\; & -2\sum_{i^-} \ln(1 - \sum_k d_{i,k} f_k) \\ & -2\sum_i \sum_k N_{i,k} \ln(d_{i,k} f_k) + \text{const.}, \end{aligned} \tag{B.8}$$

where i^- means that the summation extends over stars without detected companions. The second term reduces to a single sum over detected companions because otherwise $N_{i,k} = 0$. The parameters f_k are estimated by direct minimization of (B.8). These ML estimates are very close to those given by eq. B.5.

Confidence intervals. In order to find confidence intervals on f_k or on the total companion frequency $f = \sum_k f_k$, we have to perform constrained minimization of (B.8) with a fixed parameter f_k^*. The curve $S(f_k^*) - S_{\rm min}$ then defines the confidence intervals, as illustrated in Fig. B.1.

References

Avni, Y., Soltan, A., Tananbaum, L., & Zamoran, C. 1980, ApJ, 238, 800

Bate, M.R., Bonnell, I.A., & Brown, V. 2002, MNRAS 336, 705

Batten A.H. 1973, Binary and multiple systems of stars (Oxford: Pergamon).

Batten, A.H., Fletcher, J.M., & McCarthy, D.G. 1989, Publ. Dom. Ap. Obs., 17, 1

Bate, M.R. & Bonnell, I.A. 1997, MNRAS, 282, 33

Brandeker, A. 2004, in: Star Formation at High Angular Resolution, Proc. IAU Symp. 221, eds. M. Burton, R. Jayawardhana, T. Bourke, IAU, p. 229

Close, L.M., Richer, H.B., & Crabtree, D.R. 1990, AJ, 100, 1968

Delgado-Donate, E.J., Clarke, C.J., & Bate, M.R. 2003, MNRAS, 342, 926

Duquennoy, A. & Mayor, M. 1991, A&A, 248, 485 (DM91)

Eggenberger, A., Udry S., & Mayor M. 2004, A&A, 417, 353

Eggleton, P. & Kisseleva-Egggleton, L. 2001, ApJ, 562, 101

Fekel, F.C. 1997, AJ, 114, 2747

Goldberg, D., Mazeh, T., Latham, D.W. et al. 2002, AJ, 124, 1132

Goldberg, D., Mazeh, T., & Latham, D.W. 2003 ApJ, 591, 397

Gontcharov, G. A., Andronova, A. A., Titov, O. A., & Kornilov, E. V. 2001, A&A, 365, 222

Halbwachs, J.L., Mayor, M., Udry, S., & Arenou, F. 2003, A&A, 397, 159

Hartkopf, W.I., Mason, B.D., Wycoff, G.L., & McAlister, H.A. 2004, Fourth Catalog of Interferometric Measurements of Binary Stars. http://ad.usno.navy.mil/wds/int4.html (INT4)

Henry, T.D. & McCarthy, D.W. 1993, AJ, 106, 773

Hopmann, J. 1973, Astron. Mitt. Wien, No. 13

Isobe, S., Noguchi, M., Ohtsubo, J. et al. 1992, PNAOJ, 2, 459

Kisseleva, L., Eggleton, P., & Mikkola, S. 1998, MNRAS 200, 292

Kroupa, P. 2001, in: Zinnecker, H., & Mathieu, R.D., eds., The formation of binary stars. Proc. IAU Symp. 200, IAU.

Kroupa, P. & Burkert, A. 2001, ApJ, 555, 945

Lang, K.R. 1992, Astrophysical data. Planets and Stars. Berlin: Springer-Verlag

Larson, R.B. 2002, MNRAS, 332, 155

Latham, D.W., Stefanik, R.P., Torres, G. et al. 2002, AJ, 124, 1144

Makarov, V.V. & Kaplan, G.H. 2005, AJ, 129, 2420

Mardling, R.A. & Aarseth, S.J. 2001, MNRAS, 321, 398

Mason, B.D., Wyckoff, G.L., Hartkopf, W.I. et al. 2001, AJ, 122, 3466

Mayor, M. & Mazeh, T. 1987, A&A, 171, 157
Melo, C.H.F., Covino, E., Alcala, J.M., & Torres, G. 2001, A&A, 378, 898.
Muterspraugh, M.W., Lane, B.F., Konacki, M. et al. 2005, A&A, in print (astro-ph/0509855)
Namouni, F. 2005, AJ, 130, 280
Nordström, B., Mayor, M., Andersen, J. et al. 2004, A&A, 419, 989 80
Pourbaix, D., Tokovinin, A.A., Batten, A.H. et al. 2004, A&A, 424, 727
Poveda, A., Allen, C., & Parrao, L. 1982, ApJ, 258, 589
Reipurth, B. 2000, AJ, 120, 3177
Richichi A., Percheron, I., & Khristoforova, M. 2004, A&A, 431, 773
Shatsky, N. & Tokovinin, A. 2002, A&A, 383, 92
Sterzik, M.F. & Durisen, R.H. 1998, A&A, 339, 95
Sterzik, M.F., Durisen, R.H., & Zinnecker, H. 2003, A&A, 411, 91
Sterzik, M.F., Melo, C.H.F., Tokovinin, A.A., & van der Bliek, N. 2005, A&A, 434, 671
Tohline, J.E. 2002, ARA&A, 40, 349
Tokovinin, A. 1997, A&AS, 124, 75 (MSC)
Tokovinin, A.A. 2000, A&A, 360, 997
Tokovinin A. 2001, in: The formation of binary stars. IAU Symp. 200, ed. H. Zinnecker & R.D. Mathieu, ASP Conf. Ser., 84
Tokovinin, A. 2004, Rev. Mex. Astron. Astrof. Conf. Ser., 21, 7
Tokovinin, A.A. & Smekhov, M.G. 2002, A&A, 382, 118
Umbreit, S., Burkert, A., Henning T. et al. 2005, ApJ, 623, 940 2005ApJ...623..940U
Udry, S., Mayor, M., & Santos, N. C. 2003, A&A 407, 369
Whelan, J.A.J. 1970, MNRAS, 149, 167
Zinnecker, H., & Mathieu, R.D., eds. The formation of binary stars. Proc. IAU Symp. 200, IAU.
Zucker, S. & Mazeh, T. 2002, ApJ, 568, L113